ELSEVIER

International Journal of Mass Spectrometry 222 (2003) 201–212

International Journal of Mass Spectrometry

www.elsevier.com/locate/ijms

Effects of oxygen and water on the resonance electron capture reactions of low electron affinity compounds

M.J. Salyards, W.B. Knighton, E.P. Grimsrud*

Department of Chemistry, Montana State University, Bozeman, MT 59717, USA

Received 27 April 2002; accepted 7 August 2002

Abstract

The reactions of the molecular anions of several low electron affinity (EA) compounds, including anthracene, quinazoline, benzophenone, quinoxaline, and azulene, with oxygen and water have been studied by pulsed high pressure mass spectrometry (PHPMS). It is shown that in the simultaneous presence of oxygen and water, these molecular anions, M^-, are rapidly destroyed and the ion, $O_2^-(H_2O)$, is rapidly formed. It is shown that the high rate with which this transition occurs can not be explained by the simplest model envisioned that is based on well-known ion molecule reactions. These results can be explained, however, by inclusion into the model of a previously uncharacterized reaction between the molecular ion–oxygen complex, MO_2^-, and water. The results reported here explain why the molecular anions of compounds that have lower EA's than that of azulene are not readily observed in electron capture ion sources of 1 atm buffer gas pressure. In addition, it is shown that the reactions characterized here lead to a state of chemical equilibrium between the M^- and $O_2^-(H_2O)$ ions within the PHPMS ion source from which the EA values of the low-EA compounds can be determined. By this method the electron affinities of anthracene, quinazoline, benzophenone, and quinoxaline are found to be 0.54, 0.56, 0.61, and 0.68 eV, respectively. (Int J Mass Spectrom 222 (2003) 201–212)

Keywords: Electron capture mass spectrometry; Low electron affinity compounds

1. Introduction

In the environmental and biomedical sciences, an ever-increasing need exists for the trace detection and analysis of specific target substances in complex samples. In meeting these needs, some of the most promising methods that have been developed have been based on the gas phase negative ionization of compounds having positive electron affinities (EA) by the simple attachment of thermal-energy electrons as symbolized by Eq. (1) [1–5].

$$e + M \rightleftharpoons M^- \quad (1)$$

Resonance electron capture (REC) reactions of this type have been shown to often occur with exceedingly large rate constants, k_1, if the buffer gas pressure within the ion source is sufficiently high so that the excited molecular anion initially formed by electron attachment is rapidly stabilized by collisions with the buffer gas molecules [6]. This accounts for the extraordinarily high sensitivity that can be obtained by methods based on REC. The most common instrumental

* Corresponding author. E-mail: grimsrud@montana.edu

1387-3806/02/$ – see front matter
PII S1387-3806(02)00991-0

forms of such methods have been the electron capture detector (ECD) [2,7–9] for gas chromatography (GC), the ion mobility spectrometer (IMS) [10], the atmospheric pressure ionization mass spectrometer (APIMS) [11–13], the ion mobility spectrometer with detection by mass spectrometry (IMS/MS) [14], and the negative chemical ionization mass spectrometer (NCIMS) [4,5,15].

In the use of these methods based on REC reactions, however, a number of associated problems have been encountered. For some classes of compounds, such as halogenated aromatic hydrocarbons, trace levels of oxygen commonly present in the buffer gas of an ion source have been shown to undergo side reactions with molecular anions formed by REC [16,17]. For other classes of compounds, such as perfluorinated aliphatic hydrocarbons, trace levels of water in the buffer gas have also been shown to cause fast side reactions with molecular anions formed by REC reactions [18]. In addition, REC reactions inherently include an elementary step called thermal electron detachment (TED) that is the reverse of Eq. (1). This reaction is particularly undesirable since it completely destroys the molecular anions of interest and the associated response to the analyte, M. The rates of TED reactions increase strongly with increased temperature and decreased EA of M so that, at commonly used ion source temperatures of about 150 °C or greater, TED typically becomes unacceptably fast for compounds having EA values of less than about 18 kcal mol^{-1} [5,19,20]. In a recent report [21], we demonstrated that the detrimental effects of the TED reaction on the REC mass spectra of some low electron affinity compounds (such as benzophenone) obtained at relatively high ion source temperatures could be overcome by the intentional addition of small amounts of silicon tetrafluoride to the ion source buffer gas. Due to a strong Lewis acid–base interaction between SiF_4 and the molecular anions of low-EA compounds that have a sterically unhindered Lewis base site, a strong molecular anion–SiF_4 complex is formed which prevented the TED reaction for low-EA compounds.

Another means of minimizing the TED reaction of low-EA compounds would be expected to be offered by simply lowering the temperature of the ion source [5]. In this way, a point should be reached where the lifetime of the molecular anion against TED would be long relative to its lifetime against normal ion loss processes (either recombination with positive ions or diffusion to the walls) and the mass spectra thereby produced should include an intense molecular anion. However, when using ion sources of relatively high pressure, as in APIMS or IMS, along with relatively low ion source temperatures, we have found great difficulty in observing the expected molecular anions of low-EA compounds. For example, in spite of numerous attempts to observe and study the molecular anions of benzophenone, anthracene, and azulene, we have observed a molecular anion only for the case of azulene [22], even with use of ion source temperatures as low as 20 °C. It is interesting to note that similar observations were also made about 25 years ago by Horning et al. [23], the first practitioners of APIMS.

In recent additional observations of our own by IMS/MS, we have also noted that when low-EA compounds, such as benzophenone and anthracene, are added to the ion source at relatively low temperatures, the intensity of an ion at $m/z = 50$ is significantly increased. Since a likely assignment for the identity of this ion is $O_2^-(H_2O)$, this observation suggests that if molecular anions are being produced in these cases, they are being rapidly destroyed by reactions involving trace levels of oxygen and water, both of which commonly have partial pressures approaching the mTorr level in the buffer gases of 1 atm total pressure. In the present study, this possibility is explored in detail and is, indeed, shown to explain the lack of REC responses to low-EA compounds in high pressure ion sources at low ion source temperatures. This study also reveals a novel mechanism for the reaction of molecular anions with water and oxygen that is shown to be uniquely fast for low-EA compounds. It is also shown that the new reaction processes revealed here offers a simple and reliable means for determinating the EA of compounds having EA's less than about 0.7 eV.

2. Experimental

A pulsed high pressure mass spectrometer (PHPMS) was used for all experiments. The PHPMS was constructed in our laboratory and has been described in detail previously [18,21,24]. For the present experiments, a gaseous mixture consisting of small quantities of water, oxygen, and the low-EA compound of interest, M, were added to the major diluent gas, methane, in an associated gas handling plant. This mixture then flowed slowly through the ion source of the PHPMS. The ion source pressure was set to some constant value between 1 and 4 Torr. The ion source temperature was generally held constant at 50 °C. A brief pulse (20 μs) of 3000 eV produced positive ions and electrons within the ion source. In the methane buffer gas, these secondary electrons were rapidly thermalized and then captured primarily by the compound M (Eq. (1)) to form molecular anions, M^-, which are also rapidly brought to thermal energy by collisions with the buffer gas. At the relatively low temperature used, the primary loss of these M^- ions will not be by their TED reactions, but will be shown to be by reactions with oxygen and water. The number density of ions within the source is sufficiently low so that the dominant loss of total negative charge is by diffusion to the ion source walls rather than by recombination with positive ions [25]. Relative ion abundances within the ion source are determined as a function of time after the e-beam pulse by measuring the relative ion wall currents; that is, by observing the ions that pass through a narrow slit on one wall of the ion source into a vacuum chamber where the ions are mass analyzed (quadrupole mass filter), detected (ion-counting channeltron), and time analyzed (multichannel scaler).

3. Results and discussion

In order to mimic the absolute concentrations of water and oxygen that might commonly be present in an ion source at 1 atm pressure, small amounts of water (0.9 mTorr) and oxygen (0.5 mTorr) were added to the methane buffer gas (3.0 Torr) of our PHPMS.

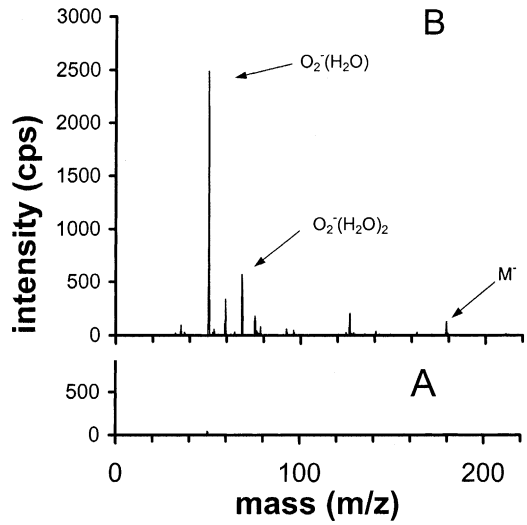

Fig. 1. (A) The negative ion mass spectrum obtained with 0.5 mTorr oxygen and 0.9 mTorr water present in the methane buffer gas of the PHPMS ion source. The total pressure is 3.0 Torr and the ion source temperature is 50 °C. (B) The negative ion spectrum obtained immediately after 0.06 mTorr anthracene was also added to the ion source mixture described in (A).

The negative ion mass spectrum thereby produced is shown in Fig. 1A. At the attenuation setting used for this mass spectrum, a very weak signal is noted at $m/z = 50$, presumed to be due to the negative ion, $O_2^-(H_2O)$. This ion was possibly formed by the REC reaction of O_2, followed by the hydration of the resulting O_2^- ion by water. The observed low intensity of this ion can be attributed to the very low rate constant for the REC reaction by oxygen. The pseudo second-order rate constant for the attachment of thermal energy electrons to oxygen at 50 °C in nitrogen buffer gas at 3.0 Torr pressure is estimated to be only about 1×10^{-13} $cm^3\,s^{-1}$ [26], which is about six orders of magnitude slower than the rate constants of fast REC processes (e.g., those of numerous substituted nitrobenzene compounds are known to exceed 1×10^{-7} $cm^3\,s^{-1}$ [6]).

The mass spectrum shown in Fig. 1B was then obtained after adding 0.06 mTorr of anthracene to the same gas mixture that was used to produce the spectrum in Fig. 1A. Under these conditions, it is noted that only a small amount of the molecular anion,

M^-, for anthracene at $m/z = 178$ is detected. The much more important effects of anthracene's addition are noted for the ions of lower mass, which are not materially related to anthracene. The most abundant of these is the ion at $m/z = 50$, again thought to be $O_2^-(H_2O)$, and the next most abundant ion at $m/z = 68$ is thought to be $O_2^-(H_2O)_2$. An ion of low intensity at $m/z = 60$ is thought to be due to CO_3^- which is probably also formed from $O_2^-(H_2O)$ by its reaction with trace levels of CO_2 in the buffer gas. An ion of minor abundance at $m/z = 126$ is thought to be due to presence of an unknown impurity possibly introduced with anthracene. Finally, an ion at $m/z = 210$ is also invariably observed with anthracene and oxygen simultaneously present in the ion source, although the intensity of this ions is very low under the specific conditions of the experiment shown in Fig. 1B. This ion is thought to be due to an anthracene–oxygen adduct ion, MO_2^-. In summary, the effects of adding anthracene on the spectrum in Fig. 1B are roughly those which we have been typically observed whenever anthracene or other compound of similarly low EA has been introduced to an atmospheric pressure ion source set to a relatively low temperature. That is, instead of observing an intense M^- ion, as expected, the intensity of the $O_2^-(H_2O)$ ion is greatly increased.

3.1. Determination of the mechanism

In order to obtain information concerning the dynamics of the reactions which produced the unexpected spectrum shown in Fig. 1B, measurements of relative ion intensities were also made as a function of time after the e-beam pulses. Again using the case of anthracene as an example, one set of measurements of this type is shown in Fig. 2. Under the conditions of reagent concentrations used in this case, the molecular anion of anthracene, M^-, is the major ion initially formed by its REC reaction immediately after the e-beam pulse. However, within only about 2 ms after the pulse, the relative abundance of M^- has been decreased to a terminal level of about 0.30 and that of the $O_2^-(H_2O)$ ion has increased to a terminal level of about 0.55. Over this short period of time, an O_2^- ion

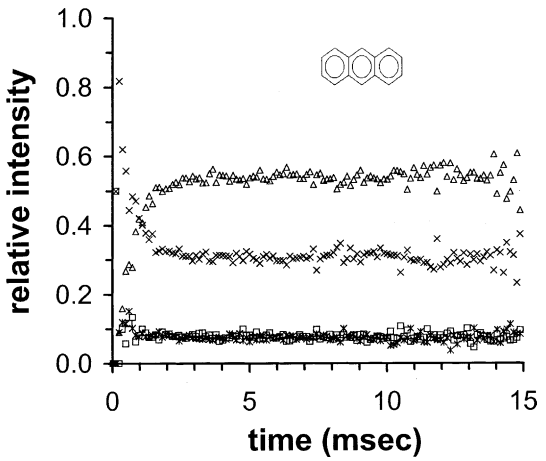

Fig. 2. PHPMS measurements of the relative intensities of the major ions, M^- (×), O_2^- (∗), MO_2^- (□), and $O_2^-(H_2O)$ (△), observed as a function of time after the e-beam pulse with 0.80 mTorr oxygen, 0.050 mTorr water, and 0.17 mTorr anthracene present in the ion source. The total methane buffer gas pressure is 3.0 Torr and the ion source temperature is 50 °C.

and the anthracene–oxygen adduct ion, MO_2^-, have also each reached terminal levels of about 0.07. Over the entire period from about 2 to 10 ms after the pulse, either a state of chemical equilibrium or a steady dynamic state appears to have been reached in which the relative abundances of these four ions remain constant.

In attempting to identify the detailed reactions and mechanism that produced spectrum in Fig. 1B and the time dependencies shown in Fig. 2, it is appropriate to first consider the most obvious candidate which is primarily based on well-known negative ion-molecule reactions. This mechanism will be referred to here as "Model A" and consists of the series of reactions shown below which are assumed to occur immediately after the molecular anion, M^-, has been formed by the e-beam pulse and Eq. (1).

$$M^- + O_2 \rightleftharpoons M + O_2^- \quad (2)$$

$$O_2^- + H_2O \rightleftharpoons O_2^-(H_2O) \quad (3)$$

$$M^- + O_2 \rightleftharpoons MO_2^- \quad (4)$$

Eq. (2) is a simple electron transfer from the molecular anion to oxygen. The rate constants for the

forward and reverse directions can be readily estimated. The reverse reaction is expected to occur with collision frequency [27] and, therefore, will be about $k_{-2} = 2 \times 10^{-9}\,cm^3\,s^{-1}$. The rate constant for the forward reaction can be estimated from k_{-2} and the equilibrium constant, $K_2 = k_2/k_{-2}$, expected for this reaction which can be deduced from $K_2 = \exp(-\Delta G_2^\circ/RT)$. The standard free energy change, ΔG_2°, for Eq. (2) is adequately provided by the difference in the electron affinities of oxygen and anthracene [28]. Using a literature value of $EA_{O_2} = 0.45\,eV$ [29] and the EA of anthracene to be determined here, $EA_M = 0.54\,eV$, an estimate of $k_2 = 8 \times 10^{-11}\,cm^3\,s^{-1}$ at 50 °C is obtained using a collisional rate constant and a Boltzman exponent with an activation energy for the reaction which is equal to the difference in electron affinities. Rate constants for both the forward and reverse directions of Eq. (3) can be obtained from previous determinations of the third-order rate constant for the forward direction [30] and the total free energy change, $\Delta G_3^\circ = -11.9\,kcal\,mol^{-1}$ for this reaction at 50 °C [31]. From these, a second-order rate constant of about $k_3 = 2 \times 10^{-11}\,cm^3\,s^{-1}$ and a first-order rate constant of about $k_{-3} = 4\,s^{-1}$ are obtained under the present reaction conditions of 3.0 Torr total pressure and 50 °C. The combination of Eqs. (2) and (3) in Model A provide for the conversion of M^- to $O_2^-(H_2O)$. Eq. (4) is included in Model A in order to account for the observed production of the adduct ion, MO_2^-, and as a side reaction, is envisioned to play no role in the conversion of M^- to $O_2^-(H_2O)$ ions. In order to account for the position of equilibrium for Eq. (4) and the rapid achievement of this state observed in Fig. 2, a near collisional second-order rate constant of $k_4 = 1 \times 10^{-9}\,cm^3\,s^{-1}$ and a first-order rate constant of $k_{-4} = 8 \times 10^4\,s^{-1}$ have been assigned to the forward and reverse directions of Eq. (4), respectively, in Model A.

In order to determine whether Model A provides an adequate explanation of the dynamics of the anthracene reaction system, a computer simulation of the pulsed e-beam experiment based on Model A was created and is shown in Fig. 3. In comparing this prediction with the experimental results shown in Fig. 2,

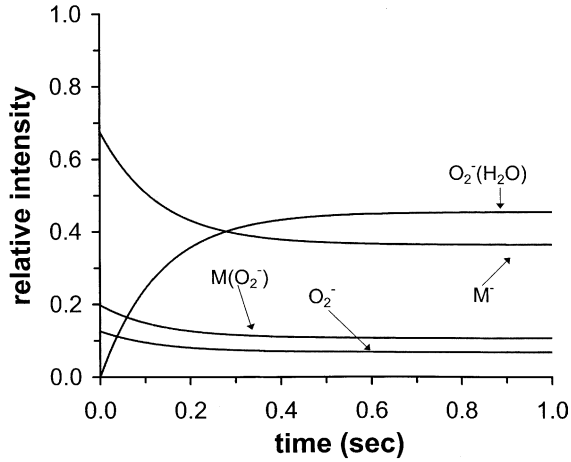

Fig. 3. The relative intensities of the major ions, M^-, O_2^-, MO_2^-, and $O_2^-(H_2O)$ predicted by the candidate mechanism, Model A, as a function of time under the ion source conditions described in Fig. 2.

it is noted that the final equilibrium state predicted by Model A is, indeed, in good agreement with the experimental results. However, it is also noted that the time required to achieve this terminal state by Model A is about 200 times longer (0.4 s) than was required in the experiment (2 ms). Therefore, Model A does not adequately describe the processes by which the M^- ions of anthracene were converted to $O_2^-(H_2O)$ ion in Fig. 2.

Another candidate mechanism, which will be referred to here as "Model B", can be envisioned simply by adding Eq. (5) to Eqs. (2), (3), and (4) of Model A.

$$MO_2^- + H_2O \rightleftharpoons O_2^-(H_2O) + M \quad (5)$$

In the new model thereby created, Eq. (4), which is very fast in the forward direction, along with Eq. (5) becomes the major means for conversion of M^- to $O_2^-(H_2O)$ ions. Eq. (5) might be viewed as a cluster exchange reaction in which a water molecule replaces the molecule, M, in the MO_2^- complex ion. It is driven by the expected stronger hydration of the O_2^- ion relative to that of the very charge delocalized M^- ion. An interesting point concerning Eq. (5) is that if the center of negative charge density within the complex ion, MO_2^-, lies within the molecule M

rather than O_2 (as might be expected from the fact that $EA_M > EA_{O_2}$), then motion along the reaction coordinate towards the transition state for Eq. (5) would involve a shift in negative charge density from M to O_2 molecules within the complex ion. Alternately, it is also possible that the center of negative charge within the MO_2^- actually lies within the O_2 species, in spite of its lower EA, possibly due to the increased ion clustering potential of the molecule, M, over that of O_2.

In order to estimate rate constants for the forward and reverse directions of Eq. (5), the same procedure as was previously applied to Eq. (4) will be used. That is, it is assumed that the steady-state condition which is achieved by the intermediate ion, MO_2^-, and the product ion, $O_2^-(H_2O)$, in Fig. 2 is reasonably close to an equilibrium condition for Eq. (5). With this assumption, an equilibrium constant for Eq. (5), $K_5 = k_5/k_{-5} = 25$, is determined from the measured ratio of MO_2^- and $O_2^-(H_2O)$ ion intensities in Fig. 2 at any time after $t = 2$ ms and the known concentrations of H_2O and M within the ion source. The magnitudes of k_5 and k_{-5} were then varied until the model provided the best fit to the observed time dependencies of ion intensities. With estimates of $k_5 = 2 \times 10^{-9}$ cm^3 s^{-1} and $k_{-5} = 8 \times 10^{-11}$ cm^3 s^{-1}, and using the same rate constants as used in Model A for Eqs. (2), (3), and (4), the time dependencies predicted by Model B are shown in Fig. 4 to be in very good agreement with the experimental results in Fig. 2. In summary, while Eqs. (2) and (3) must be occurring and account for the steady-state abundance of O_2^- observed in this case, they are of minor importance in the observed fast conversion of M^- ions to $O_2^-(H_2O)$ ions. This is thought to be caused primarily by the sequence of Eqs. (4) and (5), both of which are sufficiently fast in both directions as to cause the rapid achievement of a true equilibrium condition between these two ions.

In Fig. 5, a PHPMS experiment is shown where quinazoline rather than anthracene was used as the low-EA compound. Under these conditions, the ions M^-, MO_2^- and $O_2^-(H_2O)$ again have significant relative intensity with the MO_2^- ion being significantly more intense than it was for anthracene in Fig. 2. For this reason, much less oxygen and much more

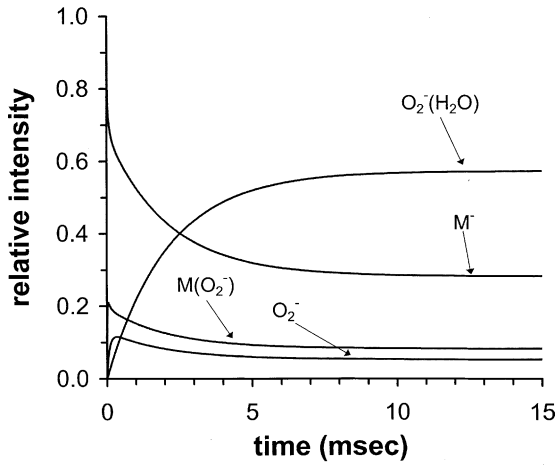

Fig. 4. The relative intensities of the major ions, M^-, O_2^-, MO_2^-, and $O_2^-(H_2O)$ predicted by the candidate mechanism, Model B, as a function of time under the ion source conditions described in Fig. 2.

water was used in this case in order have significant ion abundances of these three major ions throughout the period of measurement. Because a higher water concentration was used in this case, two higher order water cluster ions, $MO_2^-(H_2O)$ and $O_2^-(H_2O)_2$,

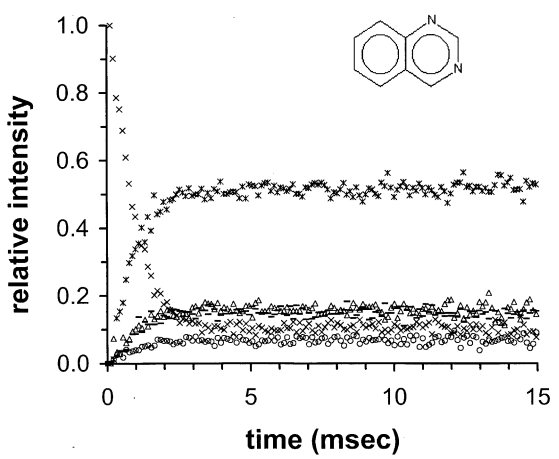

Fig. 5. PHPMS measurements of the relative intensities of the major ions, M^- (×), MO_2^- (∗), $MO_2^-(H_2O)$ (–), $O_2^-(H_2O)$ (△), and $O_2^-(H_2O)_2$ (○), observed as a function of time after the e-beam pulse with 0.15 mTorr oxygen, 1.06 mTorr water, and 0.38 mTorr quinazoline present in the ion source. The total methane buffer gas pressure is 3.0 Torr and the ion source temperature is 50 °C.

Table 1
Electron affinities of low-EA compounds and rate constants for elementary steps in mechanistic models

Compound	k_2 ($cm^3\,s^{-1}$)	k_{-2} ($cm^3\,s^{-1}$)	k_4 ($cm^3\,s^{-1}$)	k_{-4} (s^{-1})	k_5 ($cm^3\,s^{-1}$)	k_{-5} ($cm^3\,s^{-1}$)	EA (eV; present study)	EA (eV; literature)
Anthracene	7.8×10^{-11}	2×10^{-9}	1×10^{-9}	8.2×10^{4}	1×10^{-9}	4.0×10^{-11}	0.54	0.53 [33], 0.60 [34]
Quinazoline	3.8×10^{-11}	2×10^{-9}	4×10^{-10}	3.6×10^{2}	2.2×10^{-10}	2×10^{-9}	0.56	0.58 [35]
Benzophenone	6.4×10^{-12}	2×10^{-9}	1×10^{-10}	6.5×10^{3}	5×10^{-10}	5×10^{-10}	0.61	0.62 [27], 0.65 [36], 0.64 [37]
Quinoxaline	5.2×10^{-13}	2×10^{-9}					0.68	0.71 [35]

also have significant relative intensities in Fig. 5. In this case, the O_2^- ion does not have significant relative abundance because much less oxygen was used and because the rate constant, k_2, will be smaller than it was for anthracene due to the slightly greater EA for quinazoline (0.56 eV), as indicated in Table 1. In Fig. 5, it is again seen that the time required for establishment of constant relative ion intensities is very short, about 2 ms. Application of Model A to this reaction system predicts that about 0.5 s would be required to achieve this terminal state and, therefore, Model A again fails to explain this reaction system. However, when Eq. (5) is also included in the mechanism for quinazoline, excellent agreement between the experimental results and those predicted by Model B are obtained when values of $k_5 = 2 \times 10^{-10}$ cm^3 s^{-1} and $k_{-5} = 2 \times 10^{-9}$ cm^3 s^{-1} are assigned (note that for this case, it is the reverse direction of Eq. (5) that appears to occur with near collision frequency). In order to account for the two higher order water cluster ions observed in this case, rate constants for the forward and reverse water clustering reactions were set to 4.6×10^{-11} cm^3 s^{-1} and 4.9×10^3 s^{-1}, respectively, values which have been previously determined specifically for the clustering reaction leading to $O_2^-(H_2O)_2$ at 50 °C [30].

In Fig. 6, a PHPMS experiment using benzophenone (EA = 0.61 eV) as the low-EA compound is shown. In this case and under these experimental conditions, only the M^-, MO_2^- and $O_2^-(H_2O)$ ions have major relative abundance. Again, a steady-state condition is very quickly achieved, within about 1 ms after the e-beam pulse. Again, this fact can not be explained in terms of Model A by which this state is predicted to occur only after about 0.7 s. The results in Fig. 6 are again well explained, however, by Model B when the forward and reverse rate constants shown in Table 1 are assigned to Eqs. (4) and (5).

In Fig. 7, a PHPMS experiment using quinoxaline, which has a significantly greater EA of 0.68 eV, is shown. Even though relatively high concentrations of both oxygen and water were used, it is noted that $O_2^-(H_2O)$ ions are formed somewhat more slower than for they were with use of the three compounds

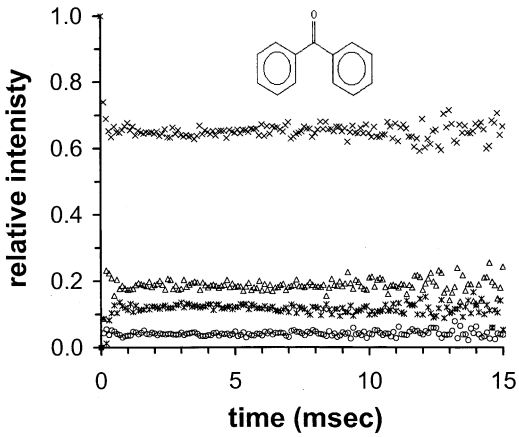

Fig. 6. PHPMS measurements of the relative intensities of the major ions, M^- (×), MO_2^- (∗) $O_2^-(H_2O)$ (△), and $O_2^-(H_2O)_2$ (○), observed as a function of time after the e-beam pulse with 0.44 mTorr oxygen, 0.95 mTorr water, and 0.86 mTorr benzophenone present in the ion source. The total methane buffer gas pressure is 3.0 Torr and the ion source temperature is 50 °C.

of lower EA previously considered. In this case, the achievement of terminal ion abundance ratios required about 5 ms. Also, it is noted that the adduct ion, MO_2^-, does not have significant relative abundance

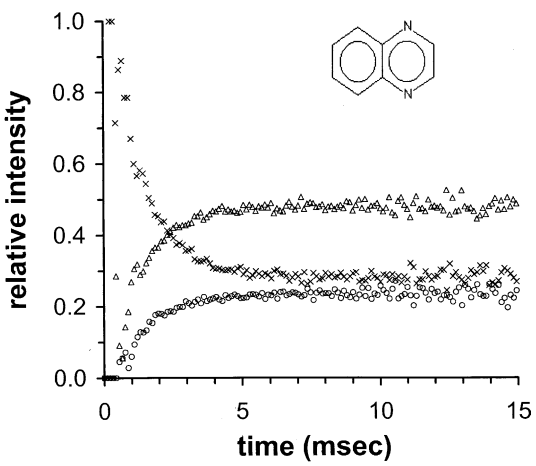

Fig. 7. PHPMS measurements of the relative intensities of the major ions, M^- (×), $O_2^-(H_2O)$ (△), and $O_2^-(H_2O)_2$ (○), observed as a function of time after the e-beam pulse with 0.98 mTorr oxygen, 1.52 mTorr water, and 0.040 mTorr quinoxaline present in the ion source. The total methane buffer gas pressure is 3.0 Torr and the ion source temperature is 50 °C.

in this case. The fact that O_2^- is not observed in this case is expected due to the higher EA of quinoxaline which shifts the equilibrium position of Eq. (2) far to the left. As with the cases previously considered, the time dependence of the ion intensities observed for quinoxaline can not be explained by Model A. Primarily because the magnitude of k_2 for this reaction system is exceedingly low, Model A predicts that about 0.6 s would be required to achieve the terminal state. Therefore, it appears that this reaction system also proceeds by a different mechanism, which might also be assumed to be Model B. In the case of quinoxaline, however, it was not possible to experimentally determine the magnitudes of the individual rate constants of the two elementary steps, Eqs. (4) and (5), from PHPMS measurements as is was in the previous cases considered because the intermediate adduct ion, MO_2^-, does not have significantly high relative intensity as to provide a reliable estimate of the equilibrium constants, K_4 and K_5.

In Fig. 8, a PHPMS experiment using azulene as the low-EA compound is shown. Azulene also has a somewhat greater EA of 0.69 eV [32] and, in addition, is known to have an usually large entropy of

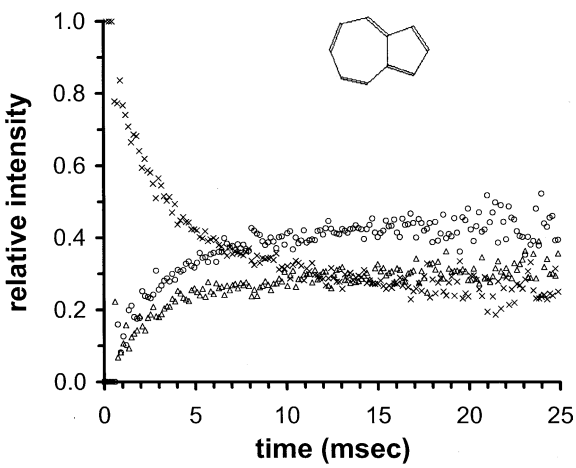

Fig. 8. PHPMS measurements of the relative intensities of the major ions, M^- (×), $O_2^-(H_2O)$ (△), and $O_2^-(H_2O)_2$ (○), observed as a function of time after the e-beam pulse with 4.8 mTorr oxygen, 4.0 mTorr water, and 0.040 mTorr azulene present in the ion source. The total methane buffer gas pressure is 3.0 Torr and the ion source temperature is 50 °C.

negative ionization ($\Delta S^\circ_{ni} = 4.5\,\text{cal}\,\text{K}^{-1}\,\text{mol}^{-1}$ [32]) which contributes about 0.08 eV additional free energy to its negative ionization at 50 °C. Under the conditions of this experiment which included very high concentrations of both oxygen and water, it is noted that $O_2^-(H_2O)$ ions were formed much more slowly than for they were for all four compounds of lower EA previously considered. After the 40-ms period of this experiment, a terminal steady-state condition was being approached but has not yet clearly been achieved. It is also noted that the adduct ion, MO_2^-, again does not have significant relative abundance in this case. The fact that O_2^- is not observed is again expected due to the higher EA and the ΔS°_{ni} of azulene, which shifts the equilibrium position of Eq. (2) far to the left. As with the cases previously considered, the time dependence of the ion intensities observed for azulene could not be explained in terms of Model A. Due primarily to the exceedingly small magnitude of k_2 (about $3 \times 10^{-14}\,\text{cm}^3\,\text{s}^{-1}$) for this case, Model A predicts that the terminal state would take almost a full second to reach. Therefore, it appears that Model B is again required to explain the slower reaction dynamics associated with azulene. For this case, the rate constants for Eqs. (4) and (5) again could not be individually estimated because the intermediate ion, MO_2^-, again did not have significant relative intensity. The results shown here for azulene differ significantly from all of those previously considered here in that even though very high oxygen and water concentrations were used, the conversion of M^- ions to $O_2^-(H_2O)$ ions proceeded too slowly as to bring this reaction system into a state of chemical equilibrium within the time of the experiment. This explains why in past studies of the electron capture reactions of low-EA compounds in buffer gases of 1 atm pressure containing trace levels of oxygen and water, the molecular anion of azulene has been easy to observe while those of compounds having slightly lower EA's have not been.

3.2. Determination of electron affinities

It has been shown above that the molecular anions, M^-, initially formed by resonance electron capture

reactions and the $O_2^-(H_2O)$ ions formed by subsequent reactions of M^- with oxygen and water can be brought into a state of chemical equilibrium within the time scale of the PHPMS experiments. The dominant processes by which this occurs has been shown to be Eqs. (4) and (5) (Model B). Therefore, an overall expression for the equilibrium condition can be written by combining Eqs. (4) and (5) as shown by Eq. (6) below:

$$M^- + O_2 + H_2O \rightleftharpoons O_2^-(H_2O) + M \quad (6)$$

Equilibrium constants K_6 (atm^{-1}) for this overall process can then be obtained from the PHPMS measurements and Eq. (7):

$$K_6 = \frac{I_{O_2^-(H_2O)} P_M}{I_{M^-} P_{O_2} P_{H_2O}} \quad (7)$$

where I_i is the relative intensity of the ion, i, after equilibrium has been achieved and P_j is the partial pressure of the substance, j, within the ion source in units of atmospheres. An expression for the free energy change of Eq. (6), ΔG_6°, can be written in terms of the single-step reactions in either candidate mechanism, Model A or B. Therefore, ΔG_6° will be given by: $\Delta G_6^\circ = \Delta G_2^\circ + \Delta G_3^\circ$. For those cases except azulene where the ΔS_{ni}° of M is of negligible magnitude, ΔG_2° will be well-approximated by the difference in electron affinities of oxygen and M, i.e., $\Delta G_2^\circ = EA_M - EA_{O_2}$. Since ΔG_3° is known [31] to be $-11.9\,kcal\,mol^{-1}$ ($-0.52\,eV$) at 50 °C and EA_{O_2} is known to be 0.45 eV [29], the electron affinity of the low-EA compound can be determined from the PHPMS measurements of the equilibrium constant, K_6, and Eq. (8):

$$EA_M = EA_{O_2} - \Delta G_3^\circ - RT \ln K_6 \quad (8)$$

In Fig. 9, the EA_M values determined in this way are shown for all four of the low-EA compounds for which a state of chemical equilibrium was achieved within the time scale of the PHPMS experiments. For each compound, many determinations of this kind were made using different combinations of concentrations for oxygen, water, and the low-EA compound. In addition, the total ion source pressure was also varied over the range from 1 to 4 Torr. As can be seen in Fig. 9, the EA values thereby determined where relatively independent of these changes in experimental conditions. From the average of these measurements, the EA values listed in Table 1 were determined for each of the four compounds. These values of 0.54, 0.56, 0.61, and 0.68 eV for anthracene, quinazoline, benzophenone, and quinoxaline, respectively, are shown to be in reasonably good agreement of the literature values also indicated in Table 1.

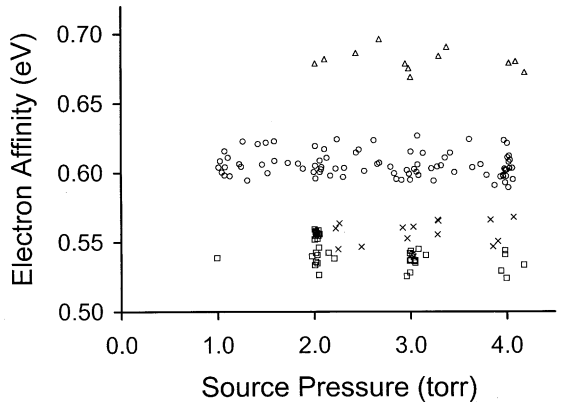

Fig. 9. Electron affinity determinations for anthracene (□), benzophenone (○), quinoxaline (△), and quinazoline (×) by the PHPMS method described here. The individual measurements shown where obtained using a variety of different reagent concentrations and total ion source pressures between 1 and 4 Torr.

The method of EA determination for low-EA compounds just described offers an advantage over the usual PHPMS method for EA determinations in which the equilibrium position of the electron transfer reaction of the compound of interest is measured against another compound of known and similar EA. In such measurements, it is often difficult to arrange the concentration ratios so that significant ion intensities are observed for both molecular anions (as in the case of Eq. (2) in the present study). With the present method and the simultaneous use of two reference compounds, oxygen and water, a given change of the concentrations of both oxygen and water results in a much greater change in the ion intensity ratio, $I_{O_2^-(H_2O)}/I_{M^-}$ (for example, lowering the concentrations of O_2 and H_2O by one order of magnitude causes an increase in the

ion intensity ratio of two orders of magnitude). In addition, with use of the conventional method based on paired low-EA compounds, the ubiquitous presence of trace oxygen and water in common buffer gas supplies give rise to the fast reactions described here which, of course, constitute unwanted side reactions in the conventional method.

4. Conclusions

In this study, we have discovered why molecular anions, M^-, for many low-EA compounds, M, are not readily observed in electron capture ion sources operating under buffer gas conditions of near ambient conditions of pressure and temperature. This is because these molecular anions react rapidly with trace levels of oxygen and water to form the ion, $O_2^-(H_2O)$. It has been shown that the conversion of M^- to $O_2^-(H_2O)$ ions proceeds by way of a two-step mechanism in which the an intermediate ion complex of the type, MO_2^-, is first formed by the reaction of M^- with oxygen. Because forward and reverse rate constants for both of the elementary steps in this mechanism are relatively large, a state of chemical equilibrium is readily achieved for the overall process and this provides a convenient means for determining the electron affinities of the low-EA compounds. By this method, the electron affinities of anthracene, quinazoline, benzophenone, and quinoxaline are shown here to be equal to 0.54, 0.56, 0.61, and 0.68 eV, respectively.

Acknowledgements

This work was supported by Grant No. CHE-9816643 from the Chemistry Division of the National Science Foundation.

References

[1] R.C. Dougherty, J. Dalton, F.J. Biros, J. Org. Mass Spectrom. 6 (1972) 1171.
[2] A. Zlatkis, C.F. Poole (Eds.), Electron Capture, Theory and Practice in Chromatography, Elsevier Science, New York, 1981.
[3] E.A. Stemmler, R.A. Hites, Electron Capture Negative Ion Mass Spectra of Environmental Contaminants and Related Compounds, VCH Publisher, New York, 1988.
[4] L.J. Sears, J.A. Campbell, E.P. Grimsrud, Biomed. Environ. Mass Spectrom. 14 (1987) 401.
[5] W.B. Knighton, L.J. Sears, E.P. Grimsrud, Mass Spectrom. Rev. 14 (1996) 327.
[6] W.B. Knighton, R.S. Mock, D.S. McGrew, E.P. Grimsrud, J. Phys. Chem. 98 (1994) 3770.
[7] M. Dressler, Selective Gas Chromatographic Detectors, Elsevier Science, New York, 1986.
[8] E.P. Grimsrud, in: H. Hill, D. McMinn (Eds.), Detectors for Capillary Chromatography, Wiley, New York, 1992, p. 83.
[9] E.P. Grimsrud, Mass Spectrom. Rev. 10 (1992) 457.
[10] G.A. Eiceman, Z. Karpas, Ion Mobility Spectrometry, CRC Press, Boca Raton, FL, 1994.
[11] E.C. Horning, M.G. Horning, D.I. Carroll, I. Dzidic, R.N. Stillwell, Anal. Chem. 45 (1973) 936.
[12] D.I. Carroll, I. Dzidic, E.C. Horning, R.N. Stillwell, Appl. Spectrosc. Rev. 17 (3) (1981) 337.
[13] A.P. Bruins, Mass Spectrom. Rev. 10 (1991) 53.
[14] K. Giles, E. Grimsrud, J. Phys. Chem. 96 (1992) 6680.
[15] E.A. Stemmler, R.A. Hites, Anal. Chem. 57 (1985) 684.
[16] I. Dzidic, D.I. Carroll, R.N. Stillwell, E.C. Horning, Anal. Chem. 47 (1975) 1308.
[17] W.B. Knighton, J.A. Bognar, E.P. Grimsrud, J. Mass Spectrom. 30 (1995) 557.
[18] W.B. Knighton, D.R. Zook, E.P. Grimsrud, J. Am. Soc. Mass Spectrom. 1 (1990) 372.
[19] E.P. Grimsrud, S. Chowdhury, P. Kebarle, J. Chem. Phys. 83 (1985) 3983.
[20] W.B. Knighton, J. Bognar, E.P. Grimsrud, Chem. Phys. Lett. 192 (1992) 522.
[21] D.H. Williamson, W.B. Knighton, E.P. Grimsrud, Int. J. Mass Spectrom. Ion Process. 206 (2001) 53.
[22] K.E. Sahlstrom, W.B. Knighton, E.P. Grimsrud, Int. J. Mass Spectrom. Ion Process. 179/180 (1998) 117.
[23] E.C. Horning, D.I. Carroll, I. Dzidic, R.N. Stillwell, in: A. Zlatkis, C.F. Poole (Eds.), Electron Capture, Theory and Practice in Chromatography, Elsevier Science, New York, 1981, p. 359.
[24] W.B. Knighton, E.P. Grimsrud, J. Am. Chem. Soc. 114 (1992) 2336.
[25] P. Kebarle, in: J.M. Farrar, W. Saunders (Eds.), Techniques for the Study of Ion Molecule Reactions, Wiley, New York, 1988, p. 221.
[26] L.M. Chanin, A.V. Phelps, M.B. Biondi, Phys. Rev. 128 (1962) 219.
[27] E.P. Grimsrud, G. Caldwell, S. Chowdhury, P. Kebarle, J. Am. Chem. Soc. 107 (1985) 4627.
[28] P. Kebarle, S. Chowdhury, Chem. Rev. 87 (1987) 513.
[29] B.K. Janousek, J.I. Brauman, in: M. Bowers (Ed.), Gas Phase Ion Chemistry, vol. 2, Academic Press, New York, 1979, p. 53.

[30] J.D. Payzant, P. Kebarle, J. Chem. Phys. 56 (1972) 3482.
[31] M. Arshadi, P. Kebarle, J. Phys. Chem. 74 (1970) 1483.
[32] S. Chowdhury, T. Heinis, E.P. Grimsrud, P. Kebarle, J. Phys. Chem. 90 (1986) 2747.
[33] J. Scheidt, R. Weinkuf, Chem. Phys. Lett. 266 (1997) 201.
[34] T. Heinis, S. Chowdhury, P. Kebarle, Org. Mass Spectrom. 28 (1993) 358.
[35] G.W. Dillow, P. Kebarle, Can. J. Chem. 67 (1989) 1628.
[36] C. Huh, C.H. Kang, H.W. Lee, H. Nakamura, M. Mishima, Y. Tsuno, H. Yamataka, Bull. Chem. Soc. Japan 72 (1999) 1083.
[37] E.C.M. Chen, W.E. Wentworth, J. Phys. Chem. 87 (1983) 45.